Mixed hyperfine and electron-phonon interaction in the Zeeman spectra of H^- local modes in CaF_2:Ho^{3+}

Glynn D. Jones and Nicholas M. Strickland*
Department of Physics and Astronomy, PB 4800, University of Canterbury, Christchurch, New Zealand
(Received 2 September 1997; revised manuscript received 12 December 1997)

Zeeman measurements are reported for the infrared absorption lines of the (X,Y) local mode of the H^- C_{4v} center for $\langle 111\rangle$-oriented CaF_2:Ho^{3+} crystals. The Zeeman shifts and splittings are analyzed in terms of mixed Ho^{3+} nuclear-hyperfine and Ho^{3+}-H^- electron-phonon interactions. [S0163-1829(98)02921-X]

I. INTRODUCTION

We present an analysis of the measured $\langle 111\rangle$-Zeeman splitting patterns of the infrared absorption lines of the (X,Y) localized modes of the C_{4v} H^- center in CaF_2:Ho^{3+}. Both the Ho^{3+} nuclear-hyperfine interaction and the electron-phonon interaction are needed to account for the observed Zeeman patterns.

C_{4v} H^- centers of trivalent rare-earth ions (R^{3+}) in CaF_2 and SrF_2 have the R^{3+} ion charge compensated by a H^- ion located in the nearest interstitial position in the (100) direction from the R^{3+} ion.[1] For these C_{4v} centers, there are two infrared absorption lines for the localized vibrational modes of the H^- ion. For CaF_2, and for the lighter rare earths in SrF_2, the lower-frequency line is the doubly degenerate (X,Y) transverse mode with the H^- vibration in the plane normal to the R^{3+}-H^- axis and the higher-frequency line is the singly degenerate (Z) longitudinal H^- vibration along the R^{3+}-H^- axis.

C_{4v} H^- centers for all Kramers R^{3+} ions and for Pr^{3+} have electronic-doublet ground states. For these centers, it is observed that the $H^-(X,Y)$ infrared line shows more than one peak. Such (X,Y) splittings are attributed to the electron-phonon interaction between the doubly degenerate ground electronic state of the R^{3+} ion and the doubly degenerate (X,Y) local-mode phonon states of the H^- ion.[2] Under this interaction, the R^{3+} electronic and H^- vibrational states are coupled to give vibronic states, with admixtures of higher energy vibronic states accounting for the observed splittings.[2] In applied magnetic fields, the vibronic energy levels shift and split to alter the (X,Y) local-mode line profiles.[3]

The C_{4v} center for Ho^{3+} is special in that the first-excited singlet electronic level lies within 2 cm^{-1} of the singlet ground state,[4] with the two singlet states being strongly coupled by the hyperfine and longitudinal Zeeman interactions. There is an independent (X,Y) local mode associated with each of the ground and first-excited states. These local modes are mixed by the electron-phonon interaction to give these two modes distinctly different energies. In applied magnetic fields, unusual Zeeman patterns are obtained from the combined effect of the electron-phonon, hyperfine, and Zeeman interactions.

In this paper, we present a detailed analysis for the Zeeman behavior of the (X,Y) mode for the C_{4v} H^- center of Ho^{3+} in CaF_2. It is observed that the (X,Y) line of this C_{4v} H^- center is split into two principal components, whose overlapping profiles indicate additional absorption transitions lie between them. In addition, two satellite lines are symmetrically located 1 cm^{-1} on each side of this main line.

The two principal components are assigned as (X,Y) local modes associated with the Ho^{3+} ground and first-excited states, with the satellite lines being the vibronic transitions between different electronic states. The additional absorption between the principal lines is attributed to unresolved hyperfine components of these two main peaks.

In applied magnetic fields, the (X,Y)-line profiles alter. These changes are interpreted as Zeeman shifts of the mixed hyperfine electron-phonon coupled states, with good agreement being obtained with simulated spectral fits.

II. EXPERIMENTAL

The CaF_2:Ho^{3+} crystals were grown by the Bridgman-Stockbarger method with an A. D. Little R. F. induction furnace. The starting materials were CaF_2 crystal offcuts from Optovac Inc. and 99.9% pure HoF_3 from Alpha Inorganics. $\langle 111\rangle$-oriented samples were cleaved from the boules and hydrogenated by heating at 850 °C in contact with molten aluminum in a $\frac{2}{3}$ atmosphere of hydrogen gas for periods up to 40 h.

10 K Zeeman infrared-absorption spectra were measured with a BioRad FTS40 FTIR spectrometer at 0.1 cm^{-1} resolution. These were ratioed against reference spectra to minimize instrumental interference fringes.

The Zeeman cryostat has a 4 T superconducting solenoid built into its helium can with a central tube in which the crystals were mounted. This eliminates the need for low-temperature infrared windows and gave crystal temperatures of 10 K, as estimated from the relative population of levels. All the Zeeman spectra were recorded for the infrared-radiation beam along the magnetic-field direction.

All Zeeman measurements were made with the magnetic field along a $\langle 111\rangle$ direction. The three orthogonal orientations of C_{4v} centers are equally inclined to this field direction giving just one magnetically equivalent site.

III. (X,Y) LOCAL-MODE SPECTRUM OF THE $C_{4v}H^-$ CENTER

For the $Ho^{3+}C_{4v}$ H^- center, the observed infrared (X,Y) local-mode lines are transitions between vibronic states con-

TABLE I. Energies (in cm^{-1}) and $|J_z\rangle$ compositions of the eleven crystal-field levels Z_i of the ground $^5I_8$ multiplet for the Ho^{3+} F^- C_{4v} center given by the crystal-field fit of Ref. 6.

Energy	Level (irrep)	$\|J_z\rangle$ composition
0.00	$Z_1(\gamma_1)$	$-0.4900(\|8\rangle+\|-8\rangle)+0.5077(\|4\rangle+\|-4\rangle)-0.0576\|0\rangle$
0.92	$Z_2(\gamma_2)$	$-0.4927(\|8\rangle-\|-8\rangle)+0.5067(\|4\rangle-\|-4\rangle)$
86.90	$Z_3(\gamma_5)$	$0.5369\|\pm7\rangle-0.8242\|\pm3\rangle-0.1094\|\mp1\rangle+0.1380\|\mp5\rangle$
120.19	$Z_4(\gamma_3)$	$-0.4947(\|6\rangle+\|-6\rangle)+0.5049(\|2\rangle+\|-2\rangle)$
136.16	$Z_5(\gamma_5)$	$0.1021\|\pm7\rangle-0.1307\|\pm3\rangle+0.3029\|\mp1\rangle-0.9381\|\mp5\rangle$
164.65	$Z_6(\gamma_4)$	$-0.5665(\|6\rangle-\|-6\rangle)+0.4228(\|2\rangle-\|-2\rangle)$
290.55	$Z_7(\gamma_1)$	$0.5061(\|8\rangle+\|-8\rangle)+0.4804(\|4\rangle+\|-4\rangle)-0.1567\|0\rangle$
294.83	$Z_8(\gamma_2)$	$-0.5062(\|8\rangle-\|-8\rangle)-0.4929(\|4\rangle-\|-4\rangle)$
452.56	$Z_9(\gamma_3)$	$-0.5046(\|6\rangle+\|-6\rangle)-0.4935(\|2\rangle+\|-2\rangle)$
474.78	$Z_{10}(\gamma_5)$	$0.4011\|\pm7\rangle+0.1974\|\pm3\rangle+0.8449\|\mp1\rangle+0.2888\|\mp5\rangle$
496.96	$Z_{11}(\gamma_1)$	$-0.0526(\|8\rangle+\|-8\rangle)-0.1060(\|4\rangle+\|-4\rangle)-0.9848\|0\rangle$
513.53	$Z_{12}(\gamma_5)$	$-0.7334\|\pm7\rangle-0.5129\|\pm3\rangle+0.4239\|\mp1\rangle+0.1284\|\mp5\rangle$
514.75	$Z_{13}(\gamma_4)$	$0.4225(\|6\rangle-\|-6\rangle)+0.5656(\|2\rangle-\|-2\rangle)$

structed from the Ho^{3+} electronic states and the H^- (100), (010), and (000) local-mode phonon states. The electron-phonon interaction produces independent energy shifts for H^- (X,Y) vibronics associated with each Ho^{3+} electronic state.

Ho^{3+} has two low-lying electronic levels comprising the $Z_1(\gamma_1)$ singlet ground state and the $Z_2(\gamma_2)$ first-excited singlet state just 1.2 cm^{-1} above. Each of these has its own (X,Y) localized mode. The two main (X,Y) lines centered at 1037.10 cm^{-1} and 1037.45 cm^{-1} are transitions associated with the Z_1 and Z_2 states, respectively. As these transitions involve no electronic excitation of the Ho^{3+} ion, which remains in the Z_1 or Z_2 state, their intensities are those of H^- local-mode vibrations.

The two weak satellite lines are centered at 1036.12 cm^{-1} and 1038.50 cm^{-1}, close to 1 cm^{-1} above and below the two main lines. As they involve simultaneous $Z_1 \leftrightarrow Z_2$ excitations of the Ho^{3+} ion, these are Ho^{3+} vibronic transitions, which acquire intensity through electron-phonon interaction admixtures with the main H^- vibrational transitions.

The energy spacing of the Z_1 and Z_2 electronic levels of the C_{4v} H^- center can be inferred from the energy spacing between these two outer weak lines at zero magnetic field and is estimated as 1.2 cm^{-1}.

A. Hyperfine-coupled electronic singlet levels of the C_{4v} center

The 100% naturally abundant isotope ^{165}Ho has a nuclear spin I of $\frac{7}{2}$ and a nuclear moment of $4.03\mu_N$. The nuclear-hyperfine constant A_8 for the $^5I_8$ multiplet has the value of 812 MHz.[5]

The two lowest levels Z_1 and Z_2 of the $^5I_8$ ground multiplet of Ho^{3+} for the C_{4v} F^- and H^- centers are two singlet states of γ_1 and γ_2 symmetry separated by an energy 2Δ. This energy separation is 1.7 cm^{-1} for the F^- center[4] and inferred to be 1.2 cm^{-1} for the H^- center.

A crystal-field analysis[6] of the energy levels of the Ho^{3+} C_{4v} F^- center gives the $|JJ_z\rangle$ composition of the thirteen levels of the $^5I_8$ multiplet listed in Table I. For the two lowest singlet levels $Z_1(\gamma_1)$ and $Z_2(\gamma_2)$, the effective angular momentum J_z between them is $\langle J_z\rangle_{1,2}=\langle Z_1|J_z|Z_2\rangle = 5.98$.

The two hyperfine states $|Z_1,I_z\rangle$ and $|Z_2,I_z\rangle$ are mixed by the dipole hyperfine interaction $A_8 I_z J_z$ through matrix elements $\langle Z_1 I_z|AJ_z I_z|Z_2 I_z\rangle = AI_z\langle J_z\rangle_{1,2}$ to give pseudoquadrupole splitting patterns spanning 3 GHz.[4]

In the presence of an applied magnetic field, the axial component of the electronic Zeeman interaction $g_L J_z \mu_B B$ causes further mixing of the two electronic singlets Z_1 and Z_2, through Zeeman matrix elements between the electronic-nuclear states $|Z_1,I_z\rangle$ and $|Z_2,I_z\rangle$. With $g_L=\frac{5}{4}$ for the $^5I_8$ multiplet and for the magnetic field B in tesla, the Zeeman matrix elements are

$$g_L\langle Z_1 I_z|J_z|Z_2 I_z\rangle\mu_B B = 5.98 g_L I_z \mu_B B = 3.49 I_z B.$$

The Zeeman splitting patterns of the pseudoquadrupole split hyperfine levels are given by the energy eigenvalues of the coupled electronic-nuclear matrix in the states $|Z_1,I_z\rangle$ and $|Z_2,I_z\rangle$ with inclusion of these Zeeman matrix elements.[7]

B. The electron-phonon interaction V_{ev}

The observed $H^-(X,Y)$ infrared transitions are between vibronic states constructed from the Z_1 and Z_2 electronic wavefunctions of Ho^{3+} and the (000), (100), and (010) H^- local-mode phonon states. Energy shifts in these vibronic states are produced by the electron-phonon interaction V_{ev} between the Ho^{3+} electronic states and the $H^-(X,Y)$ local-mode phonons. For H^- localized modes, the local-mode phonon normal coordinates are X, Y, and Z, the displacements of the H^- ion from the equilibrium position. This follows from the small mass of the H^- ion compared to other atoms of the crystal.

To terms quadratic in the phonon normal coordinates, the electron-phonon interaction $V_{\rm ev}$ has the following form for C_{4v} symmetry:[2]

$$V_{\rm ev}=f_xX+f_yY+f_zZ+\tfrac{1}{2}(g_{xx}+g_{yy})(X^2+Y^2)+\tfrac{1}{2}(g_{xx}-g_{yy})\times(X^2-Y^2)+g_{zz}Z^2+g_{xy}XY+g_{xz}XZ+g_{yz}YZ,$$

where the electronic coordinate functions f and g transform as the conjugate irreps to the respective phonon coordinate functions.

Expressed in the spherical harmonic basis, the linear terms of $V_{\rm ev}$ can be recast into the more convenient form:

$$V_{\rm ev}=f_xX+f_yY+f_zZ=-(f_+X_-+f_-X_+)+f_zZ,$$

where $f_\pm=\mp 1/\sqrt{2}(f_x\pm if_y)$ and $X_\pm=\mp 1/\sqrt{2}(X\pm iY)$.

The electronic coordinate functions f are related to the Racah tensor operators $C_m^{(n)}$ by[2]

$$f_\pm=a_{1n}\sqrt{\frac{(n+1)!}{2(n-1)!}}r^nC_{\pm1}^{(n)}\quad\text{and}\quad f_z=a_{0n}r^nC_0^{(n)},$$

where the constants a_{0n} and a_{1n} depend on the particular model chosen for the Ho^{3+}-H^- interaction [2] and $n=2,4,6$ for f-electron ions.

For the electrostatic model of a H^- ion of point-charge q interacting with a $4f$ electron of charge e a distance D away, a_{0n} and a_{1n} are[2]

$$a_{1n}=\frac{eq}{4\pi\epsilon_0D^{n+2}}\qquad a_{0n}=\frac{-(n+1)eq}{4\pi\epsilon_0D^{n+2}}.$$

C. Local-mode vibronic state combinations for the C_{4v} H^- center

For the two lowest energy electronic levels $Z_1(\gamma_1)$ and $Z_2(\gamma_2)$, the vibronic levels formed with the (000) local-mode ground state of γ_1 symmetry are $Z_1(000)$ and $Z_2(000)$ of γ_1 and γ_2 symmetry, respectively. Because $V_{\rm ev}$ necessarily transforms as γ_1, there are no electron-phonon interaction matrix elements between these $Z_1(000)$ and $Z_2(000)$ vibronic states. The energy separation of these zero-phonon vibronic levels remains 2Δ, the energy separation of the parent Z_1 and Z_2 electronic levels.

The (X,Y) local-mode states transform as the doubly degenerate γ_5 irrep of the C_{4v} group. The combinations $[\pm]=\mp 1/\sqrt{2}[(100)\pm i(010)]$ transform as irreps of the C_4 subgroup of C_{4v}, with the $[+]$ transforming as $\hat{\gamma}_3$ and $[-]$ as $\hat{\gamma}_4$.

Vibronic doublet states $Z_1[\pm]$ and $Z_2[\pm]$ of γ_5 symmetry are formed from the Z_1 and Z_2 singlet levels and the $[\pm]$ local-mode states. The vibronic states $Z_1[\pm]$ and $Z_2[\pm]$ transforms as the same $\hat{\gamma}_3$ and $\hat{\gamma}_4$ irreps as their respective $[\pm]$ local-mode states.

Energy shifts in these vibronic states can be produced by the electron-phonon interaction between vibronic states possessing the same irreps ($\hat{\gamma}_3$ or $\hat{\gamma}_4$) of the C_4 group.

Shifts of the $Z_1[\pm]$ and $Z_2[\pm]$ states can arise from the following perturbation terms:

(a) First-order perturbations of $Z_1[\pm]$ and $Z_2[\pm]$ separately, from the $(g_{xx}+g_{yy})$ and g_{zz} second-degree terms of $V_{\rm ev}$. Off-diagonal first-order terms between $Z_1[\pm]$ and $Z_2[\pm]$ are zero since the electronic coordinate operators $(g_{xx}+g_{yy})$, $(g_{xx}-g_{yy})$, and g_{xy} transform as the γ_1, γ_3, and γ_4 C_{4v} irreps, respectively, and cannot connect the $Z_1(\gamma_1)$ and $Z_2(\gamma_2)$ electronic states.

(b) Second-order perturbations of $Z_1[\pm]$ and $Z_2[\pm]$ separately, from the $f_\pm X_\mp$ and f_ZZ first-degree terms.

(c) Second-order perturbation terms between the $Z_1[\pm]$ and $Z_2[\pm]$ vibronic states, again from the $f_\pm X_\mp$ first-degree terms, giving an additional element in the first-order perturbation matrix.

The first two of these give near-uniform shifts of the $Z_1[\pm]$ and $Z_2[\pm]$ vibronic states because of the closely similar $|J_z\rangle$ compositions of the Z_1 and Z_2 electronic states.

The principal contribution is from the third mechanism. The two vibronic states are mixed by a second-order perturbation term between them, via intermediate vibronic states Φ of γ_5 symmetry:

$$EP=\sum_\Phi\frac{\langle Z_1[\pm]|V_{\rm ev}|\Phi\rangle\langle\Phi|V_{\rm ev}|Z_2[\pm]\rangle}{E_{Z_1[\pm]}-E_\Phi},$$

and this EP term is then included in the first-order matrix.

Explicitly, the EP term involves intermediate states constructed from the four Z_3, Z_5, Z_{10}, and Z_{12} electronic levels of γ_5 symmetry and the (000) and (110) vibrational states, with the contributions from (200) and (020) intermediate states summing to zero:

$$\begin{aligned}EP&=\sum_{Z_i(\gamma_5)}\frac{\langle Z_2(\gamma_2)[+]|f_-X_+|Z_i(\gamma_5^+)(000)\rangle\langle Z_i(\gamma_5^+)(000)|f_+X_-|Z_1(\gamma_1)[+]\rangle}{\hbar\omega_x-E_{Z_i(\gamma_5)}}\\&\quad+\sum_{Z_i(\gamma_5)}\frac{\langle Z_2(\gamma_2)[+]|f_+X_-|Z_i(\gamma_5^-)(110)\rangle\langle Z_i(\gamma_5^-)(110)|f_-X_+|Z_1(\gamma_1)[+]\rangle}{-\hbar\omega_x-E_{Z_i(\gamma_5)}}\\&=\frac{\hbar}{2m\omega_x}\sum_{Z_i(\gamma_5)}\frac{\langle Z_2(\gamma_2)|f_-|Z_i(\gamma_5^+)\rangle\langle Z_i(\gamma_5^+)|f_+|Z_1(\gamma_1)\rangle}{\hbar\omega_x-E_{Z_i}}+\frac{\hbar}{2m\omega_x}\sum_{Z_i(\gamma_5)}\frac{\langle Z_2(\gamma_2)|f_+|Z_i(\gamma_5^-)\rangle\langle Z_i(\gamma_5^-)|f_-|Z_1(\gamma_1)\rangle}{-\hbar\omega_x-E_{Z_i}}\\&=\frac{\hbar}{2m\omega_x}\sum_{Z_i(\gamma_5)}\langle Z_2(\gamma_2)|f_-|Z_i(\gamma_5^+)\rangle\langle Z_i(\gamma_5^+)|f_+|Z_1(\gamma_1)\rangle\left(\frac{1}{\hbar\omega_x-E_{Z_i}}+\frac{1}{\hbar\omega_x+E_{Z_i}}\right).\end{aligned}$$

Those intermediate vibronic states $\gamma_5(000)$, formed from those excited electronic states $Z_i(\gamma_5)$ whose energies are closest to the $\hbar\omega_x$ phonon energy, have the smallest energy denominators $(E_{Z_i}-\hbar\omega_x)$ and correspondingly yield the larger energy contributions.

D. Numerical estimate of *EP*

On the point-charge model, the electron-phonon parameters $a_{1n}\langle r^n\rangle\alpha$ are

$$a_{1n}\langle r^n\rangle\alpha=\frac{eq\langle r^n\rangle}{4\pi\epsilon_0 D^{n+2}}\alpha.$$

For Ho^{3+}, $\langle r^2\rangle=0.70$ a.u., $\langle r^4\rangle=1.22$ a.u., and $\langle r^6\rangle=4.54$ a.u. as extrapolated between the reported values for Dy^{3+} and Er^{3+}.[8] For the C_{4v} H^- center, the amplitude of the (X,Y) local-mode vibration is $\alpha=\sqrt{\hbar/2m\omega_x}=0.0127$ nm.

In terms of $a_{1n}\langle r^n\rangle$, $f_\pm$ has the explicit form

$$f_\pm=\sqrt{3}a_{12}\langle r^2\rangle C^{(2)}_{\pm1}+\sqrt{10}a_{14}\langle r^4\rangle C^{(4)}_{\pm1}+\sqrt{21}a_{16}\langle r^6\rangle C^{(6)}_{\pm1}.$$

Evaluation of the electron-phonon parameters for $q=e=$one electronic charge and $D=0.273$ nm yields the point-charge model values

$$a_{12}\langle r^2\rangle\alpha=51\ \text{cm}^{-1},\quad a_{14}\langle r^4\rangle\alpha=3.4\ \text{cm}^{-1},$$

$$a_{16}\langle r^6\rangle\alpha=0.47\ \text{cm}^{-1}.$$

Table II lists the $C^{(n)}_{\pm1}$ matrix elements of the Z_1 and Z_2 levels with the four Z_3, Z_5, Z_{10}, and Z_{12} levels of γ_5 symmetry. The total contribution from these four intermediate states is just 0.025 cm^{-1}. This point-charge model estimate is much too small to account for the value of 0.34 cm^{-1} required to fit the Zeeman data of Sec. IV. Because of the quadratic dependence of the second-order electron-phonon expressions on the $f_\pm$ terms of V_{ev}, any underestimate of the electron-phonon terms leads to large underestimates of EP.

The underestimate of the electron-phonon terms by the point-charge model for rare-earth ions is particularly apparent at the lutecium end of the rare-earth series. It is related to the equal lack of success of the point-charge model in estimating the axial crystal-field contributions of H^- ions in C_{4v} H^- centers.

The point-charge values of the $n=2,4,6$ crystal-field contributions of a single point-charge q ion located a distance D away are

$$B^n_0=\frac{eq\langle r^n\rangle}{4\pi\epsilon_0 D^{n+1}}.$$

Evaluation of these for Er^{3+} yields

$$B^2_0=1070\ \text{cm}^{-1},\ B^4_0=68\ \text{cm}^{-1},\ B^6_0=9\ \text{cm}^{-1}.$$

The crystal-field analysis of the Er^{3+} H^- C_{4v} center in CaF_2 (Ref. 9) gives axial crystal-field contributions of similar orders of magnitude for the $n=2,4,6$ terms:

$$B^2_0=835\ \text{cm}^{-1},\ B^4_0=1180\ \text{cm}^{-1},\ B^6_0=624\ \text{cm}^{-1}.$$

TABLE II. Matrix elements of $C^{(n)}_{\pm1}$ and matrix elements of the electron-phonon interaction term αf_+ (in cm^{-1}) for the ground- and first-excited state singlet levels $Z_1(\gamma_1)$ and $Z_2(\gamma_2)$ with the four γ_5 levels Z_3, Z_5, Z_{10}, and Z_{12} of the $^5I_8$ multiplet of the Ho^{3+} C_{4v} F^- center in CaF_2. Electron-phonon parameters scaled to fitted crystal-field parameters were adopted.

		Ho^{3+} electronic states			
Matrix elements	n	Z_3	Z_5	Z_{10}	Z_{12}
$100\langle Z_1\|C^{(n)}_1\|Z_j\rangle$	2	−5.39	3.07	−1.93	0.42
	4	0.26	−1.98	−1.94	5.14
	6	−5.99	−4.55	−1.69	5.77
$\alpha\langle Z_1\|f_+\|Z_j\rangle$		12.31	8.44	7.52	−18.62
$100\langle Z_2\|C^{(n)}_1\|Z_j\rangle$	2	4.26	4.67	−0.40	−1.48
	4	0.31	−1.78	3.03	−4.68
	6	6.99	−2.32	4.10	−4.74
$\alpha\langle Z_2\|f_+\|Z_j\rangle$		−14.11	3.58	−11.57	16.93
Energy denominators					
E_{Z_i}		87	136	475	514
$(\hbar\omega_x-E_{Z_i})$		950	901	558	523
$(\hbar\omega_x+E_{Z_i})$		1124	1173	1512	1551
Contributions to EP		0.34	−0.06	0.21	0.81
Total net value, $EP=1.3\ \text{cm}^{-1}$					

A direct comparison between these two sets of values is not entirely appropriate, as not all of the axial crystal-field contributions can be attributed to the charge-compensating H^- ion alone. The introduction of the charge-compensating H^- ion causes some displacement of the surrounding F^- ions from exact cubic symmetry.[10] Nevertheless, it is evident that the fourth and sixth degree parameters are underestimated by more than an order of magnitude with the point-charge model.

Allowance needs to be made for the corresponding point-charge model underestimation of the electron-phonon parameters $a_{1n}\langle r^n\rangle\alpha$. On the point-charge model, these electron-phonon parameters are related to the B^n_0 axial crystal-field parameters by

$$a_{1n}\langle r^n\rangle\alpha=\frac{eq\langle r^n\rangle}{4\pi\epsilon_0 D^{n+2}}\alpha=\frac{\alpha}{D}B^n_0.$$

Using these relations with the axial crystal-field parameters for the C_{4v} H^- center of Er^{3+} yields the following revised values for the electron-phonon parameters:

$$a_{12}\langle r^2\rangle\alpha=\frac{\alpha}{D}B^2_0=40\ \text{cm}^{-1},\quad a_{14}\langle r^4\rangle\alpha=\frac{\alpha}{D}B^4_0=59\ \text{cm}^{-1},$$

$$a_{16}\langle r^6\rangle\alpha=\frac{\alpha}{D}\mathrm{B}_0^6=33\ \mathrm{cm}^{-1}.$$

Table II lists the contributions to the off-diagonal matrix element EP from each of the four γ_5 levels, yielding a total of 1.30 cm^{-1}. This more than suffices to account for the required 0.34 cm^{-1} value derived from the Zeeman analysis of Sec. IV. Of the contributions to the calculated shifts, the largest is from via the Z_{12} energy level at 514 cm^{-1}. This level is closest in energy to the $\hbar\omega_x$ phonon and contributes 73% of the total calculated shift.

It is believed that the electron-phonon interaction accounts for the observed $\mathrm{H}^-(X,Y)$ local-mode line separations.

IV. CALCULATION OF THE ZEEMAN LEVELS OF THE (X,Y) LOCAL MODE

In the absence of any crystal-field wave function data for the $\mathrm{Ho}^{3+}\mathrm{C}_{4v}\ \mathrm{H}^-$ center we adopt those in Table I determined for the $\mathrm{C}_{4v}\ \mathrm{F}^-$ center.[6]

We consider the electron-phonon interaction, hyperfine, and Zeeman interaction terms between the coupled electronic-vibrational-nuclear wavefunctions. For the two zero-phonon electronic levels $|Z_1(000)I_z\rangle$ and $|Z_2(000)I_z\rangle$, the perturbation matrix is

	$\lvert Z_1(000)I_z\rangle$	$\lvert Z_2(000)I_z\rangle$
$\lvert Z_1(000)I_z\rangle$	$-\Delta$	$(A_8I_z+g_L\mu_BB)\langle J_z\rangle_{1,2}$
$\lvert Z_2(000)I_z\rangle$	$(A_8I_z+g_L\mu_BB)\langle J_z\rangle_{1,2}$	$+\Delta$

With the hyperfine, Zeeman, and electron-phonon interactions all included, the combined nuclear hyperfine and electron-phonon interaction matrix for the $|Z_1[\pm]I_z\rangle$ and $|Z_2[\pm]I_z\rangle$ (X,Y) phonon states is the same as for the $|Z_1(000)I_z\rangle$ and $|Z_2(000)I_z\rangle$ zero-phonon states, except for the extra off-diagonal term EP arising from the electron-phonon interaction

	$\lvert Z_1[\pm]I_z\rangle$	$\lvert Z_2[\pm]I_z\rangle$
$\lvert Z_1[\pm]I_z\rangle$	$-\Delta$	$(A_8I_z+g_L\mu_BB)\langle J_z\rangle_{1,2}+EP$
$\lvert Z_2[\pm]I_z\rangle$	$(A_8I_z+g_L\mu_BB)\langle J_z\rangle_{1,2}+EP$	Δ

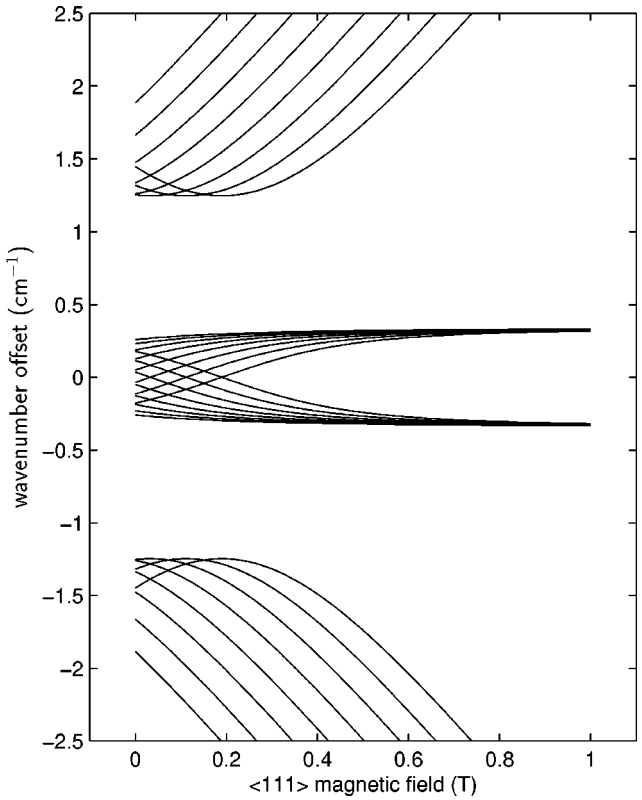

FIG. 1. Calculated magnetic-field dependence of the (X,Y) local-mode lines of the $\mathrm{C}_{4v}\ \mathrm{H}^-$ center in CaF_2:Ho^{3+}. Only those transitions which conserve I_z are shown. The 0 cm^{-1} energy identifies the energy position $\hbar\omega_x$ of the (X,Y) local mode in the absence of any electron-phonon, hyperfine or Zeeman interactions.

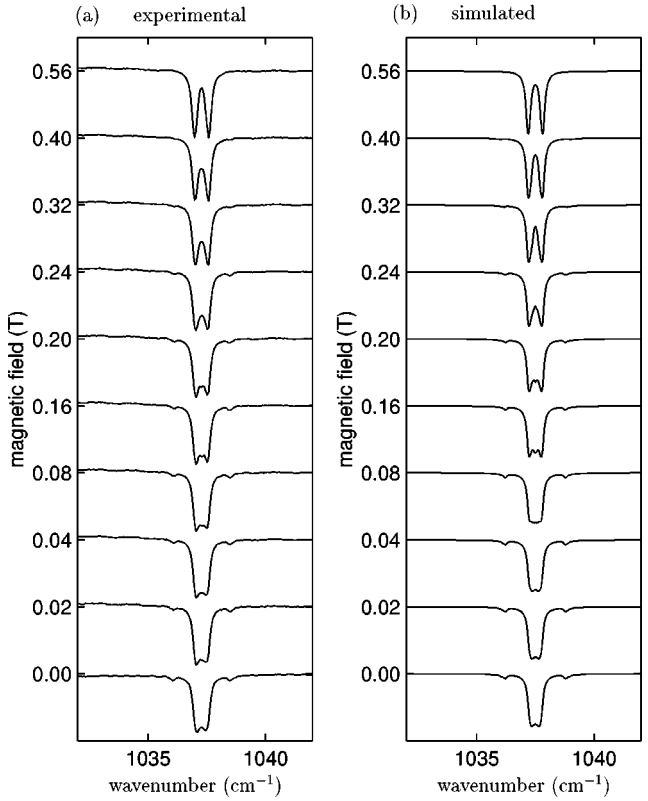

FIG. 2. Simulated and measured 10 K absorption spectra of the (X,Y) local-mode lines of the $\mathrm{C}_{4v}\ \mathrm{H}^-$ center in CaF_2:0.05%Ho^{3+} for magnetic fields along the $\langle 111\rangle$ axis. The simulated spectra are of several superposed Lorentzian lines, each with a FWHM width of 0.1 cm^{-1}.

As there is no mixing between $|I_z\rangle$ states, I_z is strictly conserved and the observed transition energies are the differences in the corresponding eigenvalues of the two matrices for the same I_z value.

A. Numerical analysis and simulation of the Zeeman patterns

The observed $\langle 111\rangle$-Zeeman patterns for which C_{4v} centers are magnetically equivalent are analyzed. For $2\Delta=1.2$ cm^{-1}, $A_8=812$ MHz, $g_L=\frac{5}{4}$, $\langle J_z\rangle_{1,2}=5.98$, and the factor $1/\sqrt{3}$ appropriate for $\langle 111\rangle$ magnetic fields, the calculated magnetic-field dependence of the hyperfine components of the $H^-(X,Y)$ vibronic transitions is given in Fig. 1. Only those transitions that conserve I_z are plotted.

In the high magnetic-field limit, the central group of transitions coalesce into two peaks. The numerical value of the electron-phonon parameter EP is equal to half the splitting between these two peaks, giving $EP=0.34$ cm^{-1}, which is the value adopted for the calculations.

The correspondence of the experimental Zeeman patterns to the calculated pattern confirms the origin of the electron-phonon energy shifts. Only the presence of the off-diagonal EP term can account for the appearance of two distinct spectral peaks in the high magnetic-field limit.

B. Intensity analysis of the $H^-(X,Y)$ local-mode profiles

The transition intensities can be obtained from the eigenfunctions of the two perturbation matrices. It is assumed that the two purely vibrational main peaks have unit intensity and that the two outer weak lines involving $Z_1 \leftrightarrow Z_2$ transitions have zero intensity for the zero vibronic-mixing limit. The observed intensities of the outer weak lines are therefore solely attributed to vibronic mixing between the Z_1 and Z_2 levels.

The relative transition strengths derived from the eigenfunctions of the two perturbation matrices are used for the simulated spectra shown in Fig. 2. Lorentzian line profiles of 0.1 cm^{-1} full width at half maximum (FWHM) were adopted for these 0.1 cm^{-1} resolution limited spectra.

The excellent agreement between the experimentally measured and the simulated spectra give confidence in the mixed hyperfine-electron-phonon interaction origin of these (X,Y) line profiles.

V. CONCLUSIONS

This electron-phonon interaction model was very satisfactorily tested by Zeeman measurements of the Ho^{3+} $H^-(X,Y)$ local-mode lines. Both the Ho^{3+} nuclear-hyperfine interaction and the electron-phonon interaction were needed to account for the observed (X,Y) line-profile changes with magnetic field.

ACKNOWLEDGMENTS

This research was supported by the University of Canterbury and the New Zealand Lottery Board through research grants. We wish to thank W. G. Smith and other technical personnel of the Department for assistance.

*Present address: Department of Physics, Montana State University, Bozeman, Montana 59717.

[1] G. D. Jones, S. Peled, S. Rosenwaks, and S. Yatsiv, Phys. Rev. **183**, 353 (1969).

[2] I. T. Jacobs, G. D. Jones, K. Zdansky, and R. A. Satten, Phys. Rev. B **3**, 2888 (1971); A. Edgar, G. D. Jones, and M. R. Presland, J. Phys. C **12**, 1569 (1979).

[3] G. D. Jones, J. Lumin. **58**, 20 (1994).

[4] P. A. Forrester and C. F. Hampstead, Phys. Rev. **126**, 923 (1963); A. A. Antipin, I. D. Livanova, and L. Y. Shekun, Fiz. Tverd. Tela **10**, 1286 (1968) [Sov. Phys. Solid State **10**, 1025 (1968)]; J. P. D. Martin, T. Boonyarith, N. B. Manson, M. Mujaji, and G. D. Jones, J. Phys.: Condens. Matter **5**, 1333 (1993).

[5] A. Abragam and B. Bleaney, in *Electron Paramagnetic Resonance of Transitions Ions* (Dover, New York, 1986), p. 298.

[6] M. Mujaji, G. D. Jones, and R. W. G. Syme, Phys. Rev. B **46**, 14 398 (1992).

[7] Z. Hasan, Solid State Commun. **73**, 109 (1990).

[8] A. J. Freeman and R. E. Watson, Phys. Rev. **127**, 2058 (1962).

[9] N. J. Cockroft, D. Thompson, G. D. Jones, and R. W. G. Syme, J. Chem. Phys. **86**, 521 (1989).

[10] D. Kiro and W. Low, in *Magnetic Resonance*, edited by C. K. Coogan, N. S. Ham, S. N. Stuart, J. R. Pilbrow, and G. V. H. Wilson (Plenum, London, 1970), p. 247; D. P. Burum, R. M. Shelby, and R. M. Macfarlane, Phys. Rev. B **25**, 3009 (1982).